Cell Reports, Volume *31*

Supplemental Information

Individual Control and Quantification of 3D Spheroids in a High-Density Microfluidic Droplet Array

Raphaël F.-X. Tomasi, Sébastien Sart, Tiphaine Champetier, and Charles N. Baroud

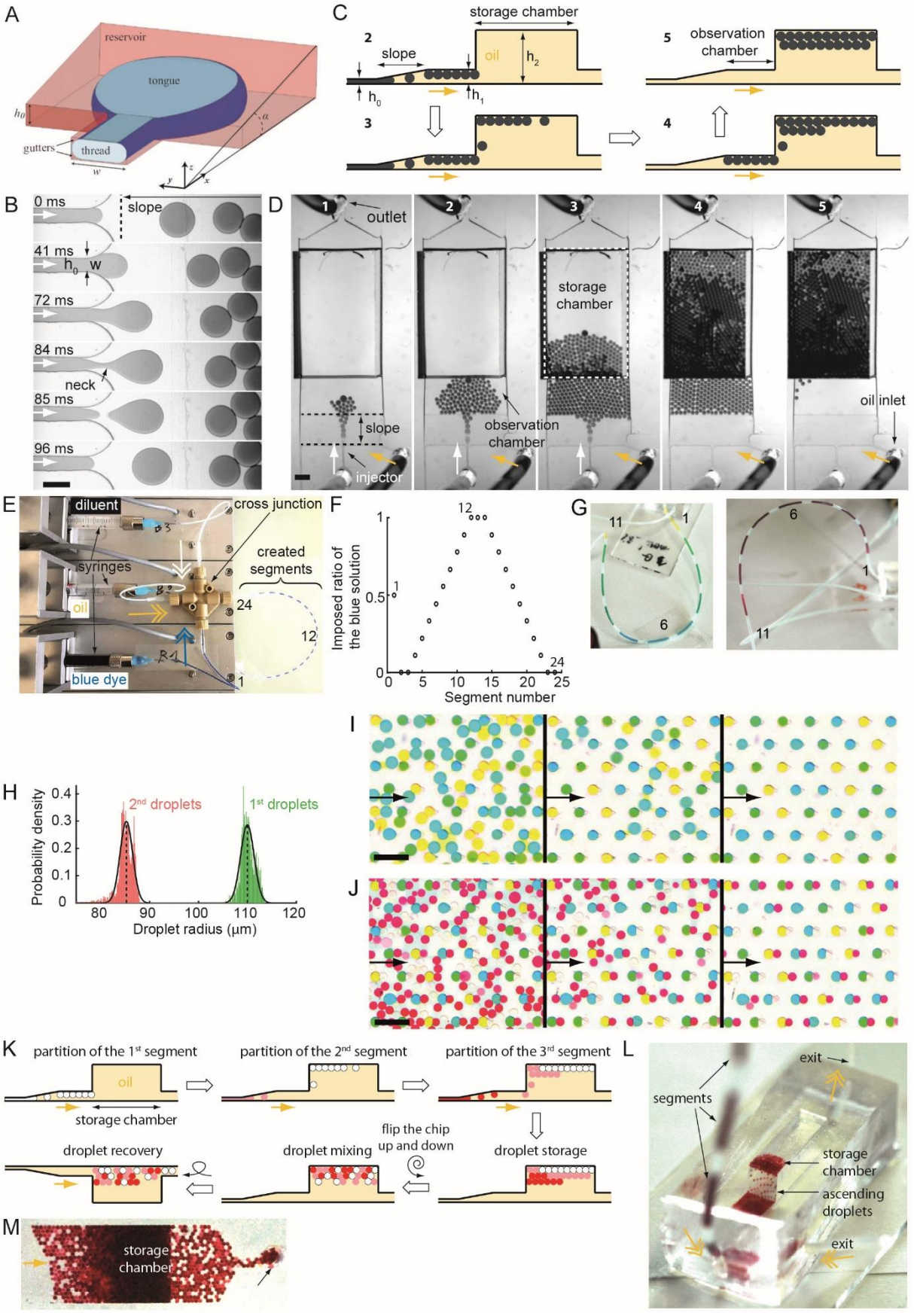

Figure S 1 : Droplet library production. Related to Figure 2. (A-D) Producing droplets with a slope. (A) Representation of a droplet production in a slope forming an angle α with the chamber floor (reproduced from (Dangla, Kayi, and Baroud 2013)). The injector has a height h_0 and a width w. (B) Time lapse images of the droplet

production (α = 8 %, h_0 = 40 µm, w = 100 µm). The dashed line represents the beginning of the slope and the white arrows represent the aqueous flowrate. Scale bar is 200 µm. (C) Schematic side view of the microfluidic chip during the droplet production. Yellow arrows represent the oil flowrate that helps the droplets entering the storage chamber. h_1 = 300 µm and h_2 = 5 mm are respectively the heights of the observation and trapping chambers. (D) Time lapse images of the chip displayed in (C). Step 2 to 5 correspond to the protocol shown in (C). Scale bar is 1 mm. (E-M) Droplet library production and injection. (E) Image of the experimental setup for the production of segmented flows with different concentrations by controlling the flowrates and volumes injected at a cross junction. (F) Graph showing the imposed ratio of the blue solution in (E) with the segment number. The segments 1, 12 and 24 are highlighted in the image (E). (G-J) Sequential filling of the anchor array with food dye droplet libraries (see Figure 2). (G) Image of the first (left) and second (right) segments before the droplet production. Segments 1,6 and 11 are highlighted on both images. (H) Polydispersity histogram of the droplets produced in the first (green; $n_{droplets}$ = 1,334; mean = 85.0 µm; CV = 1.6 %) and second (red; $n_{droplets}$ = 2,001; mean = 110.1 µm; CV = 1.3 %) droplet producing chips for a continuous injection. Black lines are Gaussian fits of the data. (I-J) Time lapse images of the first (I) and second (J) droplet trapping in 46 double anchors. The black arrows represent the direction of the oil flowrate. Scale bars are 1 mm. (K-M) Partition of the segmented flows and droplet mixing. (K) Scheme of the protocol showing a side view of the droplet production chip at every step. The spiral arrow indicates that the chip is flipped several times to ensure a good mixing of the droplets in the storage chamber. (L) Image of an experiment showing the production of the droplets from the segments. (M) Top bottom view of a droplet production chip during the droplet recovery after mixing in the storage chamber. Yellow arrows represent the oil flowrate.

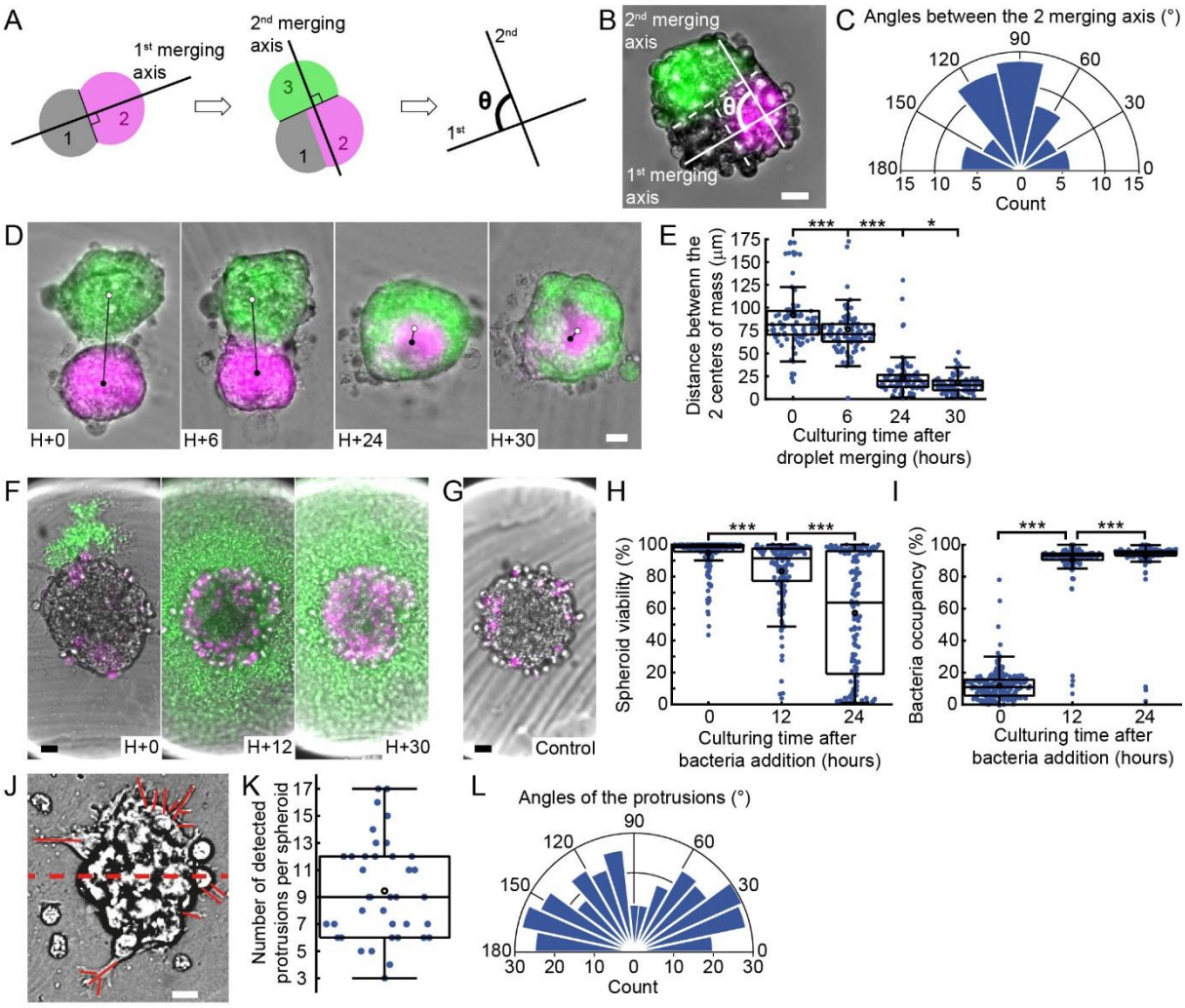

Figure S 2 : Quantification of 3D microenvironments in droplets. Related to Figure 3. (A) Scheme of the spheroid merging process. Each sequential addition of a spheroid defines a new merging axis and θ is the angle between the first and second merging axis. (B) H4-II-EC3 heterospheroids after 5 days of culture (see Figure 3C-D) with their merging axis. Dashed lines show the separation between the colored cells and white lines represent the merging axis orthogonal to the dashed lines. (C) Distribution of the angles between these merging axis (n = 56 spheroids). (D) Micrographs showing the merging between a CD146bright hMSC spheroid (magenta) and a CD146dim hMSC spheroid (green, see Figure 3E). H+0 corresponds to the hour following the droplet merging. Black and white dots represent respectively the center of mass (calculated from the spheroid fluorescent intensity) of the CD146+ and CD146- spheroids. The black line shows the distance between these 2 centers of mass. (E) Evolution of the distances between the centers of mass of the 2 hMSC spheroids (n = 94 spheroids). (F-G) Micrographs of H4-II-EC3 spheroids through time from the addition of E.coli (MG1655-GFP - green) bacteria (F, see Figure 3G) and after 2 days of culture without bacteria (G). The PI fluorescent signal is shown in magenta. Control spheroids had a mean viability of 98.0 % after 2 days of culture (n = 243 spheroids). Propidium iodide fluorescence is shown in magenta. (H-I) Evolution of the viability of the H4-II-EC3 exposed to bacteria (H) and of the bacteria occupancy (I) – proportion of the droplet projected area occupied by bacteria - through time (n = 154 spheroids). (J) B16-F0 spheroid after 1 day of culture in a Matrigel droplet (see Figure 3H-I). Visible protrusions are highlighted in red. The red dashed is the reference axis for determining the angles of each protrusion. (K-L) Distribution of the number of protrusion per spheroid (K, n = 38 spheroids) and of the protrusions angles (L, n = 338 protrusions). All scale bars are 20 µm. *: $p < 0.05$; **: $p < 0.01$; ***: $p < 0.001$. Statistical test details are provided in Table S2.

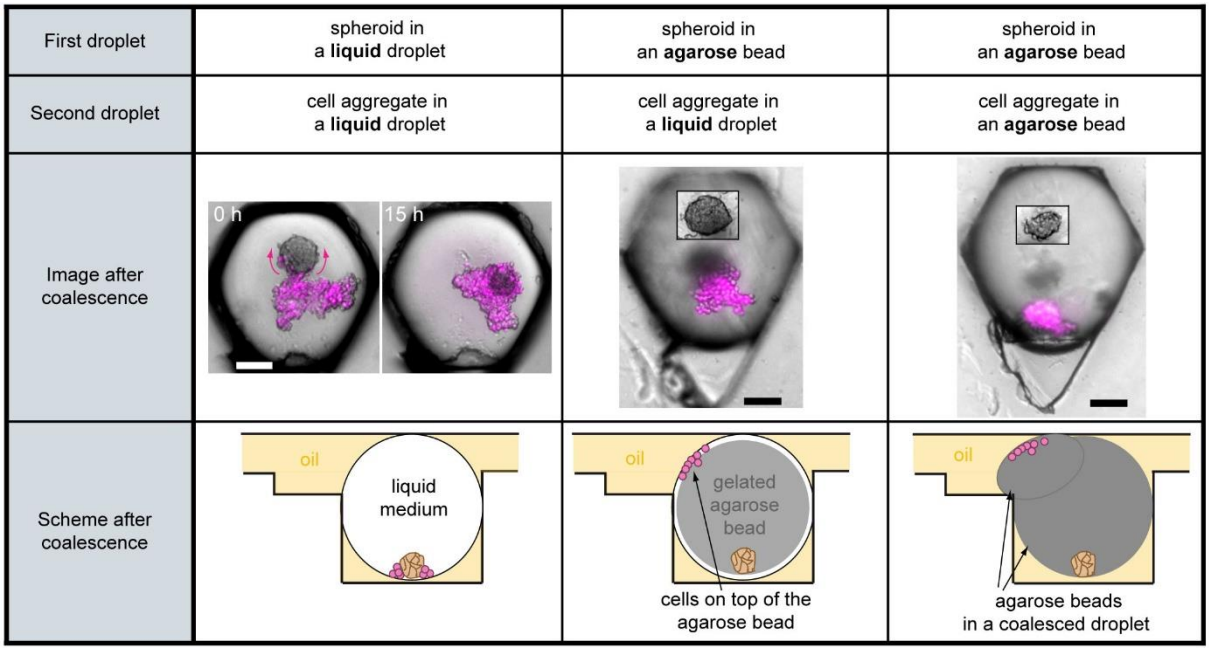

Figure S 3 : Different co-culture protocols based on droplet coalescence. Related Figure 3. In the first case (left column), the first droplet only contained cells in liquid medium. After spheroid formation, a second droplet containing other cells is trapped and merged with the first one, right after the cell sedimentation step, allowing the formation of a non-reorganized cell aggregate. The two corresponding images show one representative anchor right after (left) and 15 hours (right) after the coalescence. In the second (middle column) and third case (right column), the first droplet is gelled after the spheroid formation. The second droplet is either liquid (middle column) or gelled after cell sedimentation (right column) and merged with the first droplet immediately after capture. The two bright field insets show the first spheroid in focus at the bottom of the final droplet. In all cases, the cells brought in the second droplet were stained with CellTracker Red. Scale bars are 100 µm.

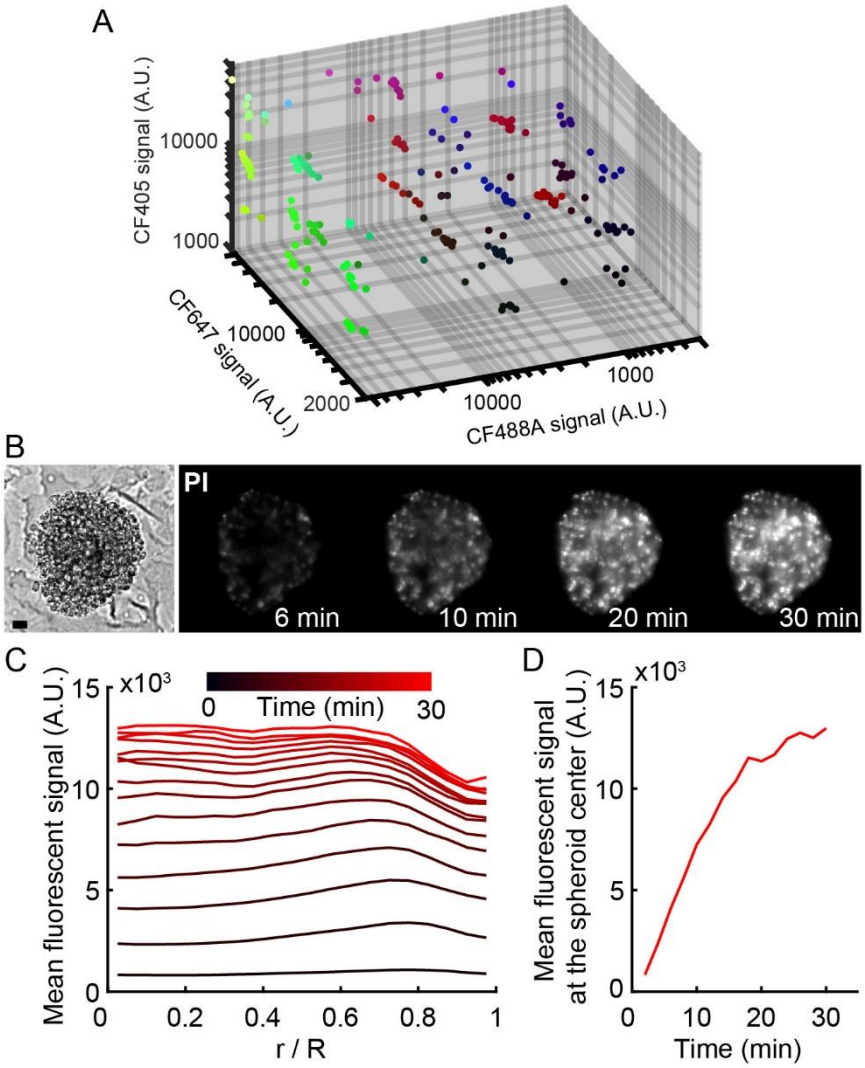

Figure S 4 : Droplet barcoding and PI diffusion. Related to Figure 4. (A) Droplet barcoding assignment. 3D scatter plot in the color space where each dot corresponds to one droplet in the picture of Figure 4C. The CF405, CF488A and CF647 fluorescent signals are shown respectively in blue, green and red for the dot colors. The barcode is made of all possible combinations of 3 concentrations of the 3 dyes : 3x3x3 = 27 barcodes. (B-D) Diffusion of the PI in the spheroids. (B) Bright field (left) and PI (right) images at different times after the beginning of the PI staining. Scale bar is 20 µm. (C) Average profile of the PI fluorescent signal over time with the normalized distance r / R to the spheroid center. The time interval between each colored curve is 2 min. (D) Evolution of the PI signal at the center of the spheroids through time. n = 42 spheroids.

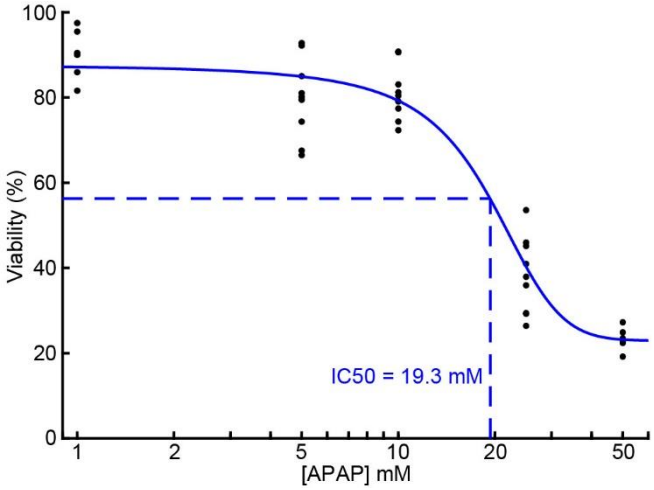

Figure S 5 : Acetaminophen (APAP) toxicity on H4-II-EC3 cell cultured in 2D. Related to Figure 5. Each black dot represent the viability calculated on 1 image. At least 6 images were acquired and analyzed for each concentration. The blue curve represents a sigmoidal fit of the data.

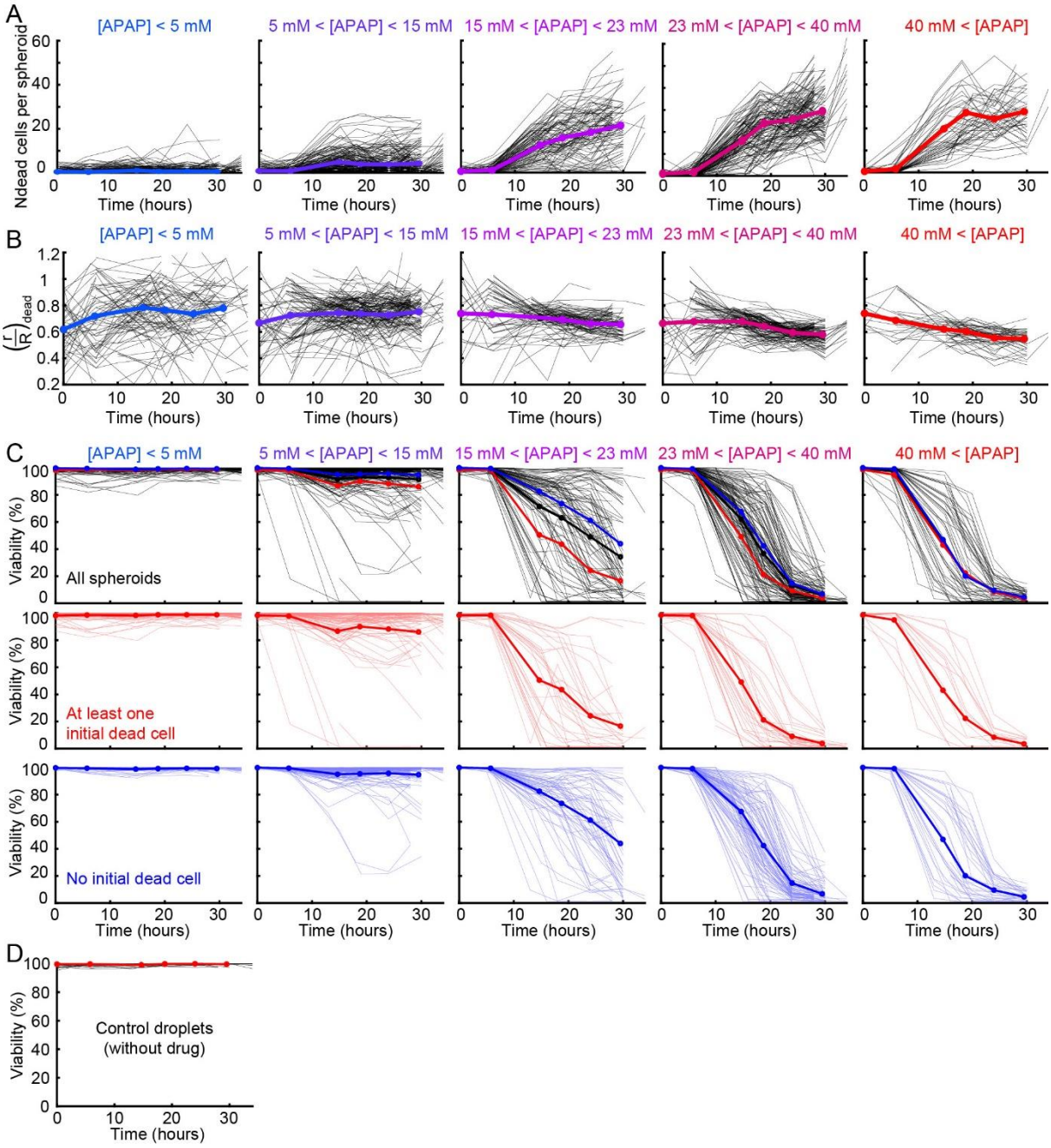

Figure S 6 : (A-B) Dynamic evolution at the spheroid level with the APAP concentration. Related to Figure 5. Evolution of the number of detected dead cell per spheroid image (A) and of the mean normalized distance of the dead cells to the spheroid center (B) with time. Each black curve represents one spheroid, the colored curves show the mean (from blue to red: [APAP] < 5 mM, $n_{spheroids}$ = 203; 5 m < [APAP] < 15 mM, $n_{spheroids}$ = 215; 15 m < [APAP] < 23 mM, $n_{spheroids}$ = 98; 23 m < [APAP] < 40 mM, $n_{spheroids}$ = 127; 40 m < [APAP], $n_{spheroids}$ = 53). (C-D) Dynamic evolution of the spheroid viability with the APAP concentration. Related to Figure 6. (C) Evolution of the spheroid viability for different APAP concentration ranges with time. The thick lines represent the mean behaviors, each black curve represents one spheroid, the red and blue curves correspond respectively the spheroids that had at least one detected dead cell and no detected dead cell at t = 0 h. [APAP] < 5 mM, $n_{spheroids}$ = 203; 5 mM < [APAP] < 15 mM, $n_{spheroids}$ = 215; 15 mM < [APAP] < 23 mM, $n_{spheroids}$ = 98; 23 mM < [APAP] < 40 mM, $n_{spheroids}$ = 127; 40 mM < [APAP], $n_{spheroids}$ = 53. (D) Dynamic evolution of the spheroid viability for the control droplets, without APAP ($n_{spheroids}$ = 76).

Table S 1 : Flowrates for the different experiments in this study. Related to STAR Methods.

Experiment	Step	Solution	Liquid loader	Flowrate (μL/min)	Approximate delivered volume (μL)
Test experiment (Figure 2)	First droplet loading	Oil+surfactant	Chamber	25	50
		Oil+surfactant	Junction	8	13
		H_2O	Aqueous phase inlet	5	8
	Second droplet loading	Oil+surfactant	Chamber	0	0
		Oil+surfactant	Junction	35	200
		2,6-DCPIP solution	Aqueous phase inlet	1	4
	Merging of droplet pairs	Destabilizing solution	Chamber	20	200
			Junction	0	0
			Aqueous phase inlet	0	0
Combinatorial mixing of colored droplets (Figure 2)	First droplet library production	Oil+surfactant	Oil inlet	2	15
		Dye segments	Injector	6	45
	Second droplet library production	Oil+surfactant	Oil inlet	2	180
		Dye segments	Injector	0.5	45
	Injection of the first and second droplet libraries	Oil+surfactant	Chamber	50	350
		Oil+surfactant	Junction	5	35
		Droplet library	Aqueous phase inlet	3	20
	Merging of droplet pairs	Destabilizing solution	Chamber	20	200
			Junction	0	0
			Aqueous phase inlet	0	0
Co-culture experiment (Figure 3)	First droplet loading	Oil+surfactant	Chamber	80	300
		Oil+surfactant	Junction	9	35
		Cell solution	Aqueous phase inlet	8	30
	Detrapping the large droplets in the triangular parts of the anchors	Oil+surfactant	Chamber	500	250
			Junction	0	0
			Aqueous phase inlet	0	0
	Second and third droplet loading	Oil+surfactant	Chamber	0	0
		Oil+surfactant	Junction	80	400
		Cell solution	Aqueous phase inlet	2	8
	Merging of droplet pairs	Destabilizing solution	Chamber	40	300
			Junction	0	0
			Aqueous phase inlet	0	0
Toxicity experiment (Figure 4-5)	First droplet loading	Oil+surfactant	Chamber	80	300
		Oil+surfactant	Junction	9	35
		Cell solution	Aqueous phase inlet	8	30
	Detrapping the large droplets in the triangular parts of the anchors	Oil+surfactant	Chamber	500	250
			Junction	0	0
			Aqueous phase inlet	0	0
	Drug droplet library production	Oil+surfactant	Oil inlet	10	45
		Droplet segments	Injector	14	60
	Injection of the drug droplet library	Oil+surfactant	Chamber	20	200
		Oil+surfactant	Junction	20	200
		Droplet library	Aqueous phase inlet	2	20
	Merging of droplet pairs	Destabilizing solution	Chamber	40	300
			Junction	0	0
			Aqueous phase inlet	0	0

Table S 2 : Statistical tests and p-values. Related to STAR Methods.

Figure number	Assumptions	Statistical test	P-values
Figure 6B	Independent sample values	Mann-Whitney U-test with unequal sample sizes	p < 1e-4
Figure 6C	Independent sample values	Mann-Whitney U-test with unequal sample sizes	p = 0.0059
Figure 6I	Independent sample values, multiple comparisons	Kruskal-Wallis ANOVA, post-hoc procedure: Mann-Whitney U-tests with Sidak's correction	1 vs 2: p = 0.0019; 1 vs 3: p = 0.0032; 1 vs 4: p = 0.025; 2 vs 3: p = 0.7539; 2 vs 4: p = 0.0014; 3 vs 4: p = 0.0314
Figure 6J	Independent sample values, multiple comparisons	Kruskal-Wallis ANOVA, post-hoc procedure: Mann-Whitney U-tests with Sidak's correction	1 vs 2: p = 0.9577; 1 vs 3: p = 0.9995; 1 vs 4: p = 0.1958; 2 vs 3: p = 09972; 2 vs 4: p = 0.1211; 3 vs 4: p = 0.0575
Figure S2E	Independent sample values, multiple comparisons	Kruskal-Wallis ANOVA, post-hoc procedure: Mann-Whitney U-tests with Sidak's correction	1 vs 2: p = 0.0004; 2 vs 3: p < 1e-4; 3 vs 4: p = 0.0270
Figure S2H	Independent sample values, multiple comparisons	Kruskal-Wallis ANOVA, post-hoc procedure: Mann-Whitney U-tests with Sidak's correction	1 vs 2: p < 1e-4; 2 vs 3: p < 1e-4
Figure S2I	Independent sample values, multiple comparisons	Kruskal-Wallis ANOVA, post-hoc procedure: Mann-Whitney U-tests with Sidak's correction	1 vs 2: p < 1e-4; 2 vs 3: p < 1e-4